

Measurement of electrostatic potential fluctuation using heavy ion beam probe in large helical device

journal or publication title	Review of Scientific Instruments
volume	Vol.79
page range	pp.10F318-1 - 10F318-4
year	2008-01-01
URL	http://hdl.handle.net/10655/3818

doi: 10.1063/1.2971207



Measurement of electrostatic potential fluctuation using heavy ion beam probe in large helical device^{a)}

Takeshi Ido, Akihiro Shimizu, Masaki Nishiura, Haruhisa Nakano, Shinsuke Ohshima, Shinji Kato, Yasuji Hamada, Yasuo Yoshimura, Shin Kubo, Takashi Shimozuma, Hiroe Igami, Hiromi Takahashi, Kazuo Toi, and Fumitake Watanabe
National Institute for Fusion Science, Gifu 509-5292, Japan

(Presented 14 May 2008; received 12 May 2008; accepted 21 July 2008;
 published online 31 October 2008)

Heavy ion beam probe (HIBP) for large helical device (LHD) has been improved to measure the potential fluctuation in high-temperature plasmas. The spatial resolution is improved to about 10 mm by controlling the focus of a probe beam. The HIBP is applied to measure the potential fluctuation in plasmas where the rotational transform is controlled by electron cyclotron current drive. The fluctuations whose frequencies change with the time constant of a few hundreds of milliseconds and that with a constant frequency are observed. The characteristics of the latter fluctuation are similar to those of the geodesic acoustic mode oscillation. The spatial profiles of the fluctuations are also obtained. © 2008 American Institute of Physics. [DOI: 10.1063/1.2971207]

I. INTRODUCTION

Heavy ion beam probe (HIBP) is a unique tool for measuring the electrostatic potential and its fluctuation and density fluctuation in high-temperature plasmas directly and simultaneously without perturbing the plasmas. In large helical device (LHD), a HIBP using 3 MV tandem accelerator is installed^{1,2} and the potential profiles are measured.³ However, there are some difficulties from the point of view of the fluctuation measurement. The energy of the probe beam is in MeV range for the LHD-HIBP. On the other hand, the amplitude of potential fluctuations in plasmas is expected to be in the range from a few volts to hundreds of volts, and the accuracy of the energy analysis is required to be 10^{-6} – 10^{-4} . Moreover, since the path length in the plasma is long, the probing beam suffers strong attenuation and the signal intensity tends to be small. In order to improve signal to noise ratio, therefore, an ion source,⁴ transport efficiency of the beam line, a detector system have been improved. In addition to that, optimization of spatial resolution is also necessary for measuring fluctuations with small spatial structure. In this article, the method to control the spatial resolution is described, and recent results of potential fluctuation measurement are presented.

II. SPATIAL RESOLUTION OF THE LHD-HIBP

Observation region has a finite volume determined by beam width and size of a slit opening, which is referred to as a sample volume. Since it determined the spatial resolution, the control of the size of the sample volume is important for measuring the potential profile with local gradient and the potential fluctuation with small spatial structure. In previous

article,⁵ the maximum length of the sample volume by the parallel beam with the diameter of 10 mm is estimated to be 42 mm at the plasma center, which is small enough to observe a gradient of a potential profile but larger than structures of turbulence. One of the ways to reduce the size of the sample volume is to control the focus of the probe beam.

In the LHD-HIBP, doublet quadrupole lens (Q -lens) is installed and the focus of the beam can be controlled in the major radius direction and the toroidal direction independently. The width of the beam is measured in two dimensions by beam profile monitors installed upstream and downstream of the Q -lens, and the focus of the beam can be estimated. Thus, we examined the dependence of the size of the sample volume on the focus of the probe beam by use of trajectory calculations.

As for the sample volume dimension in the toroidal direction, the width of sample volume in the toroidal direction can be minimized by adjusting the toroidal focus of the beam. However, such a beam diverges downstream of the sample volume and the beam width can exceed the size of the detector and the opening of beam line components. In this article, therefore, the focal position of the beam in the toroidal direction is fixed with a minimum at the detector to avoid the loss of the secondary beam.

In order to examine effects of the focus in the major radius direction, the sample volumes formed by the beam with various focuses are calculated. The initial beam diameter is 10 mm, which is a typical value measured in experiments. Shapes of the sample volumes projected on a poloidal cross section by tracing the magnetic field line are shown in Fig. 1(a). Figure 1(b) shows dependence of a width of a sample volume on the focus in the major radius direction, where the vertical axis is the maximum width of the projected sample volume and the horizontal axis is the focal position from the injection point. The size of the sample volume reaches to the minimum value when the focal posi-

^{a)}Contributed paper, published as part of the Proceedings of the 17th Topical Conference on High-Temperature Plasma Diagnostics, Albuquerque, New Mexico, May 2008.

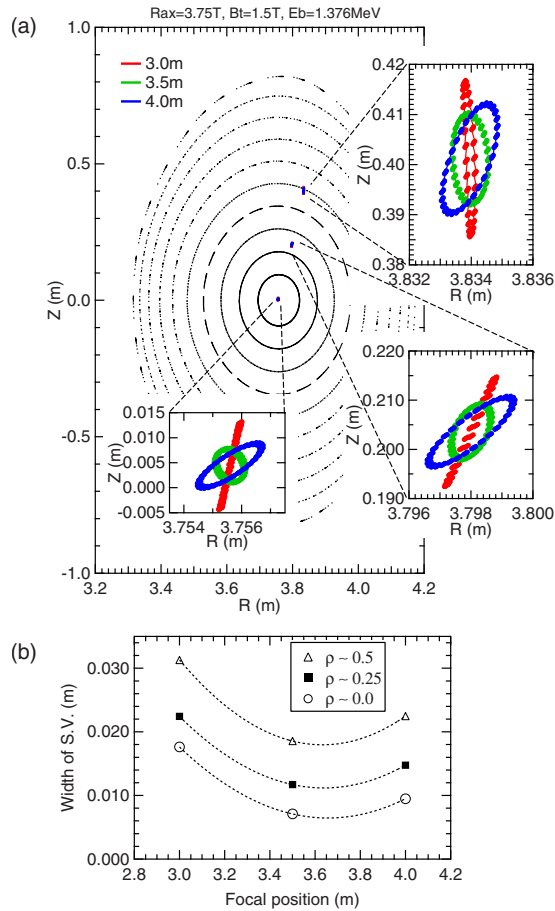


FIG. 1. (Color online) (a) Shapes of sample volumes projected on a vertically elongated poloidal cross section by tracing magnetic field lines. Only outlines of the sample volumes are drawn. The colors indicate the distance from the injection point to the focal position. (b) Dependence of the width of sample volume on the focus of the probe beam. The Horizontal axis is the distance from the injection point to the focal position in the major radius direction. Vertical axis is the maximum width of the projected sample volume.

tion is located at around 3.6 m. Optimized spatial resolutions in the poloidal cross section are 7, 11, and 19 mm in the case of measurement at $\rho \sim 0, 0.3$, and 0.5 , respectively. This is sufficient to measure fluctuations with $k\rho_i \sim 1$ in the core region using the HIBP, where k is the wave number of the fluctuation and ρ_i is the ion's Larmor radius (approximately a few tens of millimeters).

III. MEASUREMENT OF POTENTIAL FLUCTUATION

In LHD, a method to control the rotational transform by electron cyclotron current drive (ECCD) has been developed.^{6,7} Changes in the behaviors of potential fluctuations are observed using HIBP in the case of co-ECCD, by which the rotational transform is increased near the magnetic axis.

Experiments have been performed in the magnetic configuration where $B_t = 1.5$ T, $R_{ax} = 3.75$ m, $B_q = 100\%$, and $\gamma = 1.245$. Hydrogen is used as the fuel gas. The energy of the probe beam of the HIBP is 1.376 MeV. The focus of the beam is adjusted to the optimized value as shown in Sec. II. The plasma is produced and sustained by tangential neutral beam injection (NBI) from 0.4 to 2.4 s, and Co- and counter-

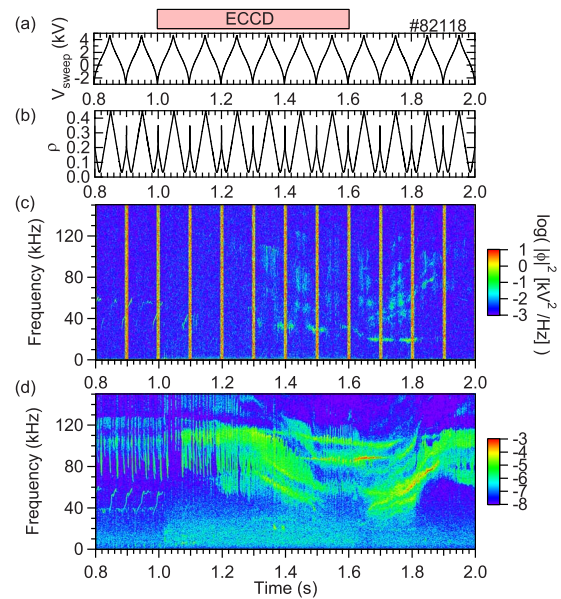


FIG. 2. (Color online) (a) Sweep voltage to control the injection angle of a beam. (b) Position of a sample volume estimated from the sweep voltage. [(c) and (d)] Frequency spectra of potential and poloidal magnetic field fluctuation, respectively. The colors indicate the common logarithm of the power.

NBI are balanced to minimize the beam-driven plasma current (Ohkawa current). ECCD is superposed from 1.0 to 1.6 s. The line integrated electron density is $0.1 \times 10^{19} \text{ m}^{-3}$, and the central electron temperatures are 4.0 and 1.0 keV with and without ECCD, respectively.

The position of the sample volume of HIBP is reciprocated from $\rho \sim 0.1$ to $\rho \sim 0.4$ at a frequency of 10 Hz. Note that the estimation of the position has the error of 0.15 in terms of ρ which is mainly caused by the misalignment due to the stray magnetic field of LHD. The frequency response of the amplifiers is improved up to 300 kHz and the sampling frequency is 1 MHz.

Figure 2(c) shows the temporal evolution of the frequency spectrum of potential fluctuation. In the NBI phase and the beginning of the superposition of ECCD (0.5–1.15 s), coherent mode whose frequency rapidly changes from 40 to 60 kHz is observed. The mode is also observed in poloidal magnetic field fluctuation in Fig. 2(d).

After the superposition of ECCD, some different modes are observed in the frequency range of 40–120 kHz from 1.3 to 1.9 s. Their frequencies change gradually with the time constant of a few hundreds of milliseconds. The behaviors of the potential fluctuations are delayed by a few hundreds of milliseconds from the timing of ECCD. The time delay probably corresponds to the time constant of the change in the current profile. In addition to that, coherent mode with the constant frequency of 32 kHz during ECCD and 19 kHz after ECCD is observed. The temperature dependence of the observed frequency is similar to that of the geodesic acoustic mode (GAM) frequency⁸ ($f_{\text{GAM}} = \sqrt{2}C_s/2\pi R_0$ for tokamaks, where C_s and R_0 are the ion sound velocity and the major radius, respectively), although the absolute values of the measured frequencies are lower than roughly predicted frequencies: 40 kHz during ECCD and 25 kHz after ECCD, where the central temperature is used as the electron tem-

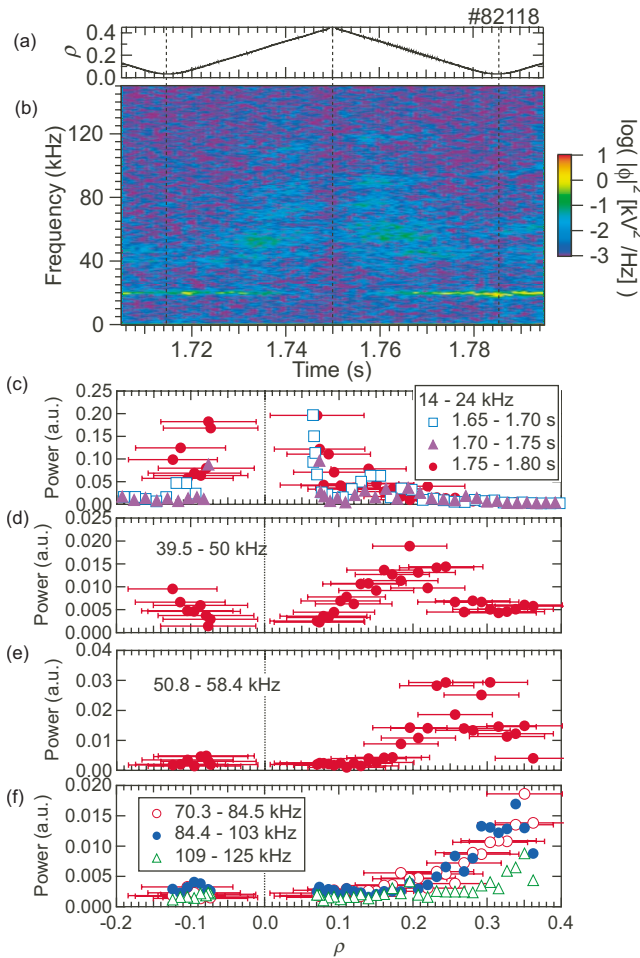


FIG. 3. (Color online) Spatial distribution of potential fluctuations. (a) Position of the sample volume. (b) Temporal behavior of the frequency spectrum of the potential fluctuation. [(c)–(f)] Power of a mode in each frequency range. The data from 1.75 to 1.80 s are analyzed in (d)–(f). Since the fluctuation in (c) shows intermittent behavior, three profiles obtained in sequential periods are drawn.

perature and the ion temperature is assumed to 0.5 keV. As shown above, the temporal behaviors of the fluctuations correlate closely with the change in the experimental conditions and the behavior of the poloidal magnetic field fluctuations. Therefore, it is concluded that the observed fluctuations are due to the plasma.

Figure 3(b) shows the expanded view of the frequency spectrum during one scan. It is a temporal evolution of the spectrum but it also includes information relating to the spatial structure because the sample volume is moving in the plasma. If the temporal variation is not significant, Fig. 3(b) can be regarded as the spatial distribution of the fluctuations. In the period, the magnetic-fluctuation signal shows all modes except the mode with the GAM frequency exists continuously, and Fig. 3(b) shows that the pattern of the spectrum except the change in the frequency is reproduced during one scan of the probing beam. Therefore, the variations in the power of the modes in Fig. 3(b) are mainly due to their spatial structures.

The observed variations in the power of the mode in each frequency range is plotted in Figs. 3(c)–3(f), where the horizontal axis is the normalized minor radius of the position

of the sample volume estimated from the sweep voltage. The profiles clearly indicate that the modes are excited at different positions locally in the plasma.

The mode with the GAM frequency is excited intermittently. To avoid misreading, three profiles obtained in sequential periods are shown in Fig. 3(c). In all periods, the fluctuation with the GAM frequency exists in the inner region of the plasma. Theoretical study^{9,10} predicts that the GAMs in helical plasmas tend to exist in the core region where the rotational transform (the safety factor) is small (large) and the damping of the GAM oscillation is mitigated. Although the mode structure is not identified yet, judging from the temperature dependence of the frequency and spatial structure, the observed fluctuation is probably a GAM oscillation.

IV. DISCUSSION

The fluctuations whose frequencies change gradually and the GAM oscillation, which are observed from 1.3 to 1.9 s in Fig. 2, are observed only in the case of co-ECCD. Thus, the excitation of the fluctuations probably depends on the profile of the rotational transform and they seem to be excited when the magnetic shear is weak or reversed. Reference 11 shows that the lowest frequency of reversed shear Alfvén eigenmode (RSAE) can become the GAM frequency, and the observed fluctuation with the GAM frequency may correspond to the RSAE with the lowest frequency. In LHD, both types of fluctuations (GAM and RSAEs) were first observed in plasmas in which the magnetic shear is reversed by neutral beam current drive.¹² The fluctuations observed during co-ECCD are inferred to be excited by same physical mechanism.

ACKNOWLEDGMENTS

We are grateful to Dr. A. Fujisawa, Dr. A. V. Melnikov, and members of the LHD experimental group for fruitful discussion. We thank Professor O. Motojima and Professor S. Sudo for their continuous encouragement. This work was supported by MEXT Japan under Grant-in-Aid for Young Scientists (Nos. 16760674 and 18760640), by the NIFS/NINS under the project of Formation of International Network for Scientific Collaborations, and by NIFS under NIFS07ULBB505, 514, and 515.

¹T. Ido, A. Shimizu, M. Nishiura, A. Nishizawa, S. Kato, T. P. Crowley, K. Tsukada, M. Yokota, H. Ogawa, T. Inoue, Y. Hamada, and the LHD Experimental Group, *Rev. Sci. Instrum.* **77**, 10F523 (2006).

²A. Shimizu, T. Ido, M. Nishiura, H. Nakano, I. Yamada, K. Narihara, T. Akiyama, T. Tokuzawa, K. Tanaka, K. Kawahata, H. Igami, Y. Yoshimura, T. Shimozuma, S. Kubo, K. Ngaoka, K. Ikeda, M. Osakabe, K. Tsumori, Y. Takeiri, O. Kaneko, S. Kato, M. Yokota, K. Tsukada, H. Ogawa, A. Nishizawa, Y. Hamada, and the LHD Experimental Group, *Plasma Fusion Res.* **2**, S1098 (2007).

³T. Ido, A. Shimizu, M. Nishiura, S. Kato, H. Nakano, A. Nishizawa, Y. Hamada, M. Yokota, K. Tsukada, H. Ogawa, T. Inoue, K. Ida, M. Yoshinuma, S. Murakami, K. Tanaka, K. Narihara, I. Yamada, K. Kawahata, N. Tamura, and LHD Experimental Group, *J. Plasma Fusion Res.* **3**, 31 (2008).

⁴M. Nishiura, T. Ido, A. Shimizu, S. Kato, K. Tsukada, A. Nishizawa, Y. Hamada, Y. Matsumoto, A. Mendenilla, and M. Wada, *Rev. Sci. Instrum.* **77**, 03A537 (2006).

⁵T. Ido, A. Shimizu, M. Nishiura, Y. Hamada, S. Kato, A. Nishizawa, and

- H. Nakano, *Plasma Fusion Res.* **2**, S1100 (2007).
- ⁶T. Shimozuma, S. Kubo, Y. Yoshimura, H. Igami, K. Nagasaki, T. Notake, S. Inagaki, S. Itoh, S. Kobayashi, Y. Mizuno, Y. Takita, K. Saito, T. Seki, R. Kumazawa, T. Watari, and T. Mutoh, *Fusion Sci. Technol.* **50**, 403 (2006).
- ⁷T. Notake, T. Shimozuma, S. Kubo, H. Idei, K. Ida, K. Watanabe, S. Sakakibara, T. Yamaguchi, M. Yoshinuma, T. Kobuchi, S. Inagaki, T. Tokuzawa, Y. Yoshimura, H. Igami, T. Seki, H. Tanaka, K. Nagasaki, and the LHD Experimental Group, *J. Plasma Fusion Res.* **3**, S1077 (2008).
- ⁸P. H. Diamond, S.-I. Itoh, K. Itoh, and T. S. Hahm, *Phys. Plasmas* **47**, R35 (2005).
- ⁹T. Watari, Y. Hamada, A. Nishizawa, and J. Todoroki, *Phys. Plasmas* **12**, 062304 (2005).
- ¹⁰S. Satake, M. Okamoto, N. Nakajima, H. Sugama, M. Yokoyama, and C. D. Beidler, *Nucl. Fusion* **45**, 1362 (2005).
- ¹¹B. N. Breizman, M. S. Pekker, S. E. Sharapov, and JET EFDA Contributors, *Phys. Plasmas* **12**, 112506 (2005).
- ¹²K. Toi, F. Watanabe, T. Tokuzawa, K. Ida, S. Yamamoto, S. Morita, S. Inagaki, S. Ohdachi, K. Narihara, S. Sakakibara, M. Osakabe, Y. Narushima, K. W. Watanabe, and LHP Experimental Group, Proceedings of the Tenth IAEA Technical Meeting on Energetic Particles in Magnetic Confinement Systems, Kloster Seeon, 2007 (unpublished).